J. Chem. Sci. Vol. 129, No. 7, July 2017, pp. 841–847. © Indian Academy of Sciences.
DOI 10.1007/s12039-017-1239-9

REGULAR ARTICLE

Special Issue on THEORETICAL CHEMISTRY/CHEMICAL DYNAMICS

Size and Structure of Cytochrome-c bound to Gold nano-clusters: Effect of Ethanol†

CATHERINE GHOSH[a], M D ASIF AMIN[a], BIMAN JANA[a] and KANKAN BHATTACHARYYA[a,b,*]

[a]Department of Physical Chemistry, Indian Association for the Cultivation of Science, Jadavpur, Kolkata, West Bengal, 700 032, India

[b]Department of Chemistry, Indian Institute of Science Education & Research Bhopal, Bhopal Bypass Road, Bhauri, Bhopal, Madhya Pradesh 462 066, India

Email: kankan.bhattacharyya@gmail.com; kankan@iiserb.ac.in

MS received 11 November 2016; revised 16 January 2017; accepted 20 January 2017

Abstract. Size and structure of cytochrome c (Cyt C) bound to gold nano-clusters (AuNC) were studied using fluorescence correlation spectroscopy (FCS) and circular dichroism (CD) spectroscopy. The CD spectra of Cyt C indicate that the ellipticity is almost completely lost on binding to AuNC which indicates unfolding. Addition of ethanol causes partial restoration of ellipticity and hence, structure of Cyt C. FCS data indicate that size (hydrodynamic radius, r_H) of free Cyt C is 17 Å which increases to 24 Å on binding to AuNC. This too suggests unfolding of Cyt C upon binding to AuNCs. Both the size and conformational relaxation time of Cyt C bound to AuNC vary non-monotonically with increase in ethanol content.

Keywords. Cytochrome c; gold nanoclusters; fluorescence correlation spectroscopy; conformational dynamics.

1. Introduction

Fluorescent metal nano-clusters have attracted a lot of attention recently because of their photo-stability, intense emission, small size, and low toxicity.[1–16] Protein-protected fluorescent metal nano-clusters have been widely used for cell imaging,[13,17] and intracellular drug and protein delivery.[14,18–20] Recently, we have used cytochrome c-protected gold nano-cluster (AuNC) to deliver cytochrome c (Cyt C) inside live cells.[19] Also, we have used lysozyme-protected AuNC for selective delivery of an anti-cancer drug to breast cancer cell without affecting normal breast cells.[14] This led to selective killing of the breast cancer cells.[14] The membrane impermeable enzyme β-galactosidase was efficiently delivered in multiple cell lines using peptide coated gold nanoparticle by Ghosh *et. al.*,[20] Liu *et. al.*, have shown that insulin retains its activity when bound to gold nanoclusters.[21]

In this work, we address the question whether a protein (Cyt C) retains its unique native structure when it binds to a metal nano-cluster. Cytochrome C is an important protein in biological system which has a significant role in apoptosis.[22,23] Cytochrome C is a charged protein, so it can strongly interact with AuNC, as a result of which the structure of the protein may be affected.

Recently, many groups have investigated the effect of binary mixtures on proteins using large scale computer simulations[24,25] and FCS.[26] Ghosh *et al.*, have explored the free energy surface of HP 36.[24] Roy *et al.*, have shown concentration dependent conformational fluctuation around active site of lysozyme in water-DMSO binary mixture.[25] Using FCS and CD spectroscopy, Chattoraj *et al.*, have found that the value of hydrodynamic radius and time scale of conformation dynamics of the protein lysozyme oscillate with variation in the concentration of ethanol in the ethanol-water mixture.[26] Amin and co-workers have reported on the effect of ethanol-water binary mixture on the structure and dynamics of cytochrome c using FCS, CD and molecular dynamics simulations.[27] In the present work, we report on the effect of ethanol-water mixture on the structure and dynamics of the protein, cytochrome c, capping the AuNC.

We have used FCS to follow the size and dynamics of Cyt C. To monitor the change in the structure of protein with various ethanol-water concentrations, we have used circular dichroism (CD) spectroscopy.

*For correspondence

† Dedicated to the memory of the late Professor Charusita Chakravarty

2. Experimental

2.1 *Materials*

Chloroauric acid ($HAuCl_4$, 30 wt% solution in dilute hydrochloric acid (99.99%, Sigma–Aldrich) and equine heart cytochrome c (Sigma–Aldrich) were used as received. Ethanol used in the experiment was of spectroscopic grade and water was of HPLC grade. C480 dye was purchased from Exciton Inc. and used without further purification.

2.2 *Methods*

2.2a *CD spectra measurement*: The CD spectroscopy was done using a JASCO J815 CD spectrometer (Model Number J-815-1505). Concentration of cytochrome c-protected gold nano-cluster used was ~4 μM. The CD spectra were recorded in the helical region (190–260 nm).

2.2b *Gold nano-cluster preparation*: Cytochrome c coated gold nanoclusters were prepared following our previously reported method.[19]

2.2c *FCS data measurement and analysis*: Our experimental setup for FCS and collection of FCS data are described in detail in our earlier publication.[28] Tween-20 (0.005%) was used to prevent attachment of the protein coated nanoclusters to the glass surface of the cover slip during the experiment. The FCS experiments were carried out at 25°C and at ~50 μW laser powers.

The FCS traces (autocorrelation function, G(τ)) have been fitted to a model involving a single component diffusion plus two component conformational relaxation (1) for ethanol concentrations upto 44.75% (v/v).[28] For ethanol concentrations greater than 44.75%, we used a bi-component diffusion equation having one component of conformational relaxation (2).

$$G_{AC}(\tau) = \frac{1}{N}\left[1+\frac{\tau}{\tau_D}\right]^{-1}\left[1+\frac{\tau}{\omega^2\tau_D}\right]^{-1/2} \times \left[1+A_1 e^{-\tau/\tau_{R1}}+A_2 e^{-\tau/\tau_{R2}}\right] \quad (1)$$

$$G(\tau) = \frac{1}{N}\left[\frac{(1-Z+Ze^{-\tau/\tau_R})}{(1-Z)}\right][\{A_1(1+\tau/\tau_{D1})^{-1} \times (1+\tau/\kappa^2\tau_{D1})^{-0.5}\} + \{A_2(1+\tau/\tau_{D2})^{-1}(1+\tau/\kappa^2\tau_{D2})^{-0.5}\}] \quad (2)$$

Where, N is the number of molecules in the observation volume, τ_{Di}'s are the diffusion time of the diffusing species, $\omega = \omega_z/\omega_{xy}$ is the ratio of longitudinal (ω_z) and transverse (ω_{xy}) radii or structure parameter of the 3D Gaussian confocal volume and τ_{Ri} is the relaxation time for an exponential component with an associated amplitude A_i.

The diffusion coefficient (D_t) is related to the diffusion time (τ_D) and transverse radius (ω_{xy}) as

$$D_t = \frac{\omega_{xy}^2}{4\tau_D} \quad (3)$$

D_t is related to hydrodynamic radius (r_H) by the Stokes Einstein equation as,

$$D_t = \frac{k_B T}{6\pi\eta r_H} \quad (4)$$

where, η, k_B, T are co-efficient of viscosity, Boltzmann constant and absolute temperature.

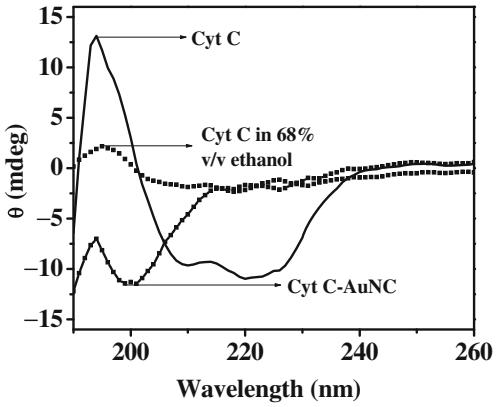

Figure 2. Circular dichroism (CD) spectra of Cyt C and Cyt C-AuNC in water and Cyt C in 68% ethanol (v/v).

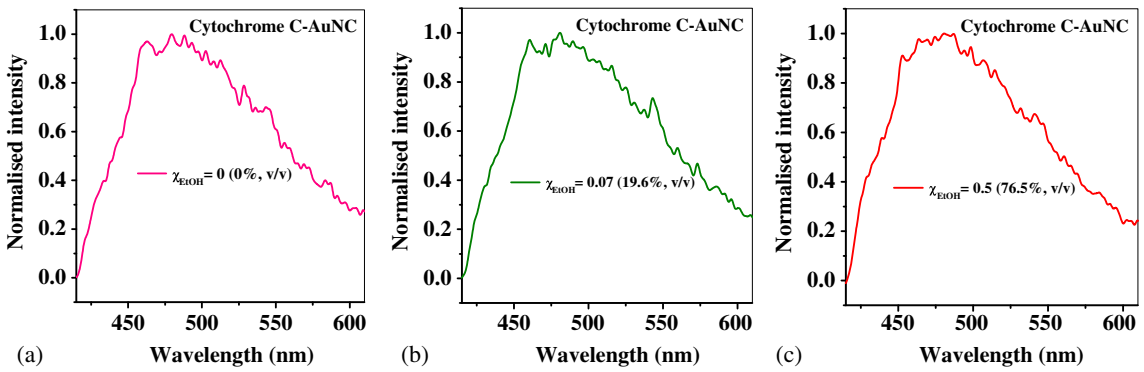

Figure 1. Emission spectra of 5 μM cytochrome c-capped AuNC at, (a) $\chi_{EtOH} = 0\%$ (v/v), (b) $\chi_{EtOH} = 19.6\%$ (v/v), (c) $\chi_{EtOH} = 76.5\%$ (v/v) ($\lambda_{ex} = 405$ nm).

FCS data analysis depends on change in refractive index of the system, laser beam geometry, *etc*.[31] The artifacts arising during FCS data analysis can be corrected in two ways. The first method involves proper alignment of the collar settings of the objective of the microscope. The second method is by using a standard dye as a calibrator of errors due to refractive index mismatch as discussed by Sherman *et al.*,[32] and Chattopadhyay *et al.*[33] We chose the second method to normalize the FCS data of the protein. We have chosen C480 as a diffusion standard and used the following equation.[30,32,33]

$$\frac{r_H^{Protein}}{r_H^{Dye}} = \frac{\tau_D^{Protein}}{\tau_D^{Dye}} \tag{5}$$

where, r_H and τ_D denote hydrodynamic radius and characteristic diffusion time, respectively.

3. Results and Discussion

3.1 *Emission spectra of cytochrome c capped AuNC*

Figures 1a–c show the emission spectra of Cyt C capped AuNC in different ethanol concentrations. The nanoclusters exhibit an emission maximum at 475 ± 2 nm. There is no change in the position of emission maximum with increase in ethanol concentration.

It may be noted that the number of Au atoms and size of the AuNCs may be calculated from the emission maxima using equation (6) (Jellium model).[19]

$$h\nu \cong \frac{E_f}{\sqrt[3]{N}} = \frac{E_f r_s}{R} \tag{6}$$

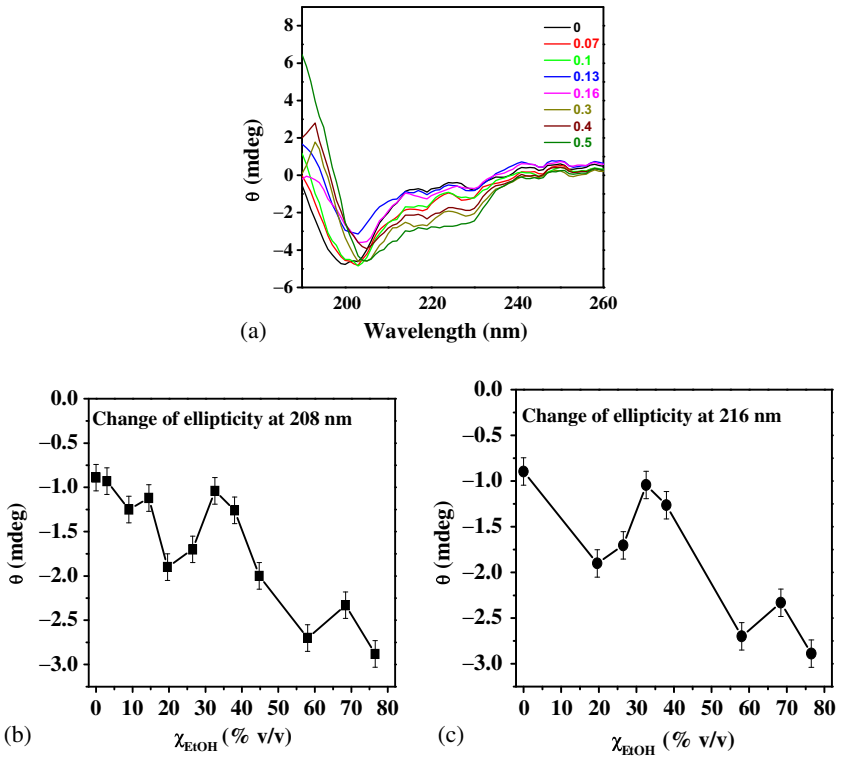

Figure 3. (a) Circular dichroism (CD) spectra, (b) ellipticity at 208 nm, and (c) ellipticity at 216 nm at various ethanol concentrations of Cyt C-AuNC.

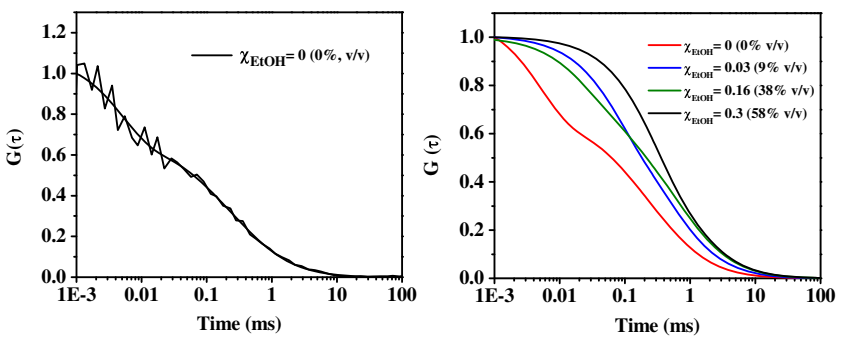

Figure 4. FCS traces of Cyt C bound to AuNC at some representative ethanol concentration.

Table 1. Hydrodynamic radius in Cyt C and Cyt C-AuNC (excluding the gold atoms) in water and 68.4% (v/v) ethanol.

System	% of EtOH (v/v)	r_{H1} (Å)*	r_{H2} (Å)*
Cytochrome c	0	17	–
	68.4	11	–
Cytochrome c bound to AuNC	0	21.6	–
	68.4	61.6 (56%)	900 (44%)

*± 2 Å

Table 2. Variation of hydrodynamic radius of Cyt C-AuNC in different ethanol concentrations.

χ_{EtOH} (mole fraction)	χ_{EtOH}(% v/v)	r_{H1} (Å)*	r_{H2} (Å)*
0	0	24	–
0.01	3	22	–
0.03	9	19	–
0.05	14.5	12	–
0.07	19.6	12	–
0.1	26.5	25	–
0.13	32.6	45	–
0.16	38	16	–
0.2	44.75	12	–
0.3	58	7 (97%)	1167 (3%)
0.4	68.4	65(56%)	900(44%)
0.5	76.5	12(78%)	3100(22%)

*± 2 Å

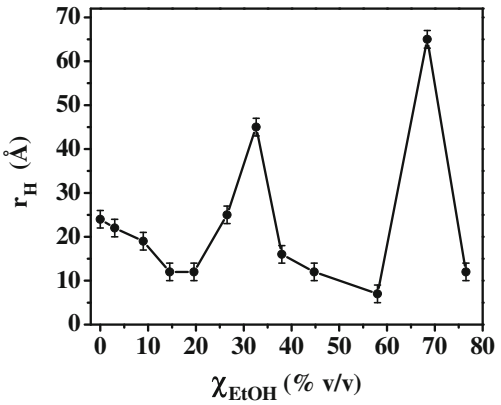

Figure 5. Variation of hydrodynamic radius (r_H) of Cyt C-AuNC in various ethanol concentrations.

where ν denotes the emission/excitation frequency, E_f, the Fermi energy, R, the radius of such nano-clusters, r_s is the Wigner-Seitz radius of the metals and N is the number of gold atoms present in the gold nanocluster.

Using the value of r_s for gold as 0.165 nm, for the given emission maximum at 475 ± 2 nm, the size of the AuNCs is calculated to be 3.5 Å using equation (6).[40] This corresponds to AuNCs having 8 Au atoms in its core. This is in good agreement with our previous study.[19] As the position of the emission maximum does not change with ethanol concentration, so neither does the size or number of Au atoms in the Cyt C-capped AuNCs.

3.2 *Circular Dichroism spectra of Cyt C in the free native state and bound to AuNC: Effect of alcohol-water mixture*

Figure 2 shows the CD spectra of cytochrome c in the native state and cytochrome c protected gold nanoclusters in water, respectively. The CD spectra of native Cyt C suggest that it exists in all α-helical form, showing two minima near 208 nm and 222 nm.[34]

From Figure 2, it is readily seen that on binding to AuNC, the CD bands around both 208 nm and 222 nm vanish and a new band arises at 200 nm. This suggests that the large scale structural changes that occur due to unfolding of Cyt C on binding to AuNC, lead to complete loss of the helical structure.

On addition of ethanol (68.4% v/v) to Cyt C (free native state) (Figure 2) the minima around 210 nm and 220 nm (due to α-helical form) vanish. This suggests that addition of ethanol to free Cyt C causes a large change in its secondary structure.

Figure 3 describes effect of ethanol on the CD spectra of Cyt C bound to AuNC. On addition of ethanol to Cyt C bound to AuNC, ellipticity around 208 nm increases (in negative direction), in general (except slight decrease around 32.6% ethanol v/v) which suggest partial re-folding of Cyt C caused by ethanol. On addition of EtOH to Cyt C bound to AuNC, the negative ellipticity at 216 nm increases which is ascribed to formation of β sheet.[35,36]

3.3 *Fluorescence Correlation Spectroscopy (FCS)*

Figure 4 gives representative FCS traces of Cyt C bound to AuNC in the absence and presence of EtOH.

FCS data gives size (hydrodynamic radius, r_H) and conformational relaxation time of a protein.[26,29,37–39] In this section, we report on the effect AuNC and subsequently ethanol on Cyt C. The FCS data could be fitted to a model having single component of diffusion and two components of conformational relaxations for ethanol concentrations up to 44.75%. Beyond this concentration, the FCS data could no longer be fitted to the above model and the data was fitted to a model with two components of diffusion and one component of relaxation.

3.3a *Size of Cyt C in free native state and bound to AuNC-effect of ethanol*: As listed in Table 1, in the absence of ethanol, radius of Cyt C is 17 Å. On addition of ethanol, it decreases to 11 Å indicating compaction or collapse of the protein.

The hydrodynamic radius (r_H) obtained from fluorescence correlation spectroscopy (FCS) of Cyt C bound to AuNC at various ethanol concentrations are given (Table 2 and Figure 5).

Table 3. Variation of time scales of conformation dynamics (τ_{R1} and τ_{R2}) of Cyt C-AuNC- in different ethanol concentrations.

χ_{EtOH} (mole fraction)	χ_{EtOH} (% v/v)	τ_{R1} (μs)*	τ_{R2} (μs)*
0	0	5 (18%)	70(82%)
0.01	3	8 (10%)	41 (90%)
0.03	9	6 (20%)	69(80%)
0.05	14.5	5 (20%)	49 (80%)
0.07	19.6	8 (30%)	48 (70%)
0.1	26.5	3 (30%)	73 (70%)
0.13	32.6	2 (20%)	90 (80%)
0.16	38	6 (60%)	133 (40%)
0.2	44.75	2 (10%)	300 (90%)
0.3	58	–	50
0.4	68.4	–	92
0.5	405	–	405

* ± 10%

Subtracting the size of the AuNC (3.5 Å, obtained using equation (6) in section 3.1), the size of the Cyt C bound to AuNC is 21.6 Å (Table 1).

From Table 2 and Figure 5, it can be seen that with the increase in χ_{EtOH} the r_H varies in an oscillatory manner. At first, with addition of alcohol the radius of protein started to decrease till 19.6% and then increases till 32.6%. Again, the size decreases till 58% and finally decreases after a sharp increase in size.

At higher ethanol concentration, the FCS curve of Cyt C bound to AuNC cannot be fitted with single diffusion component, so we fitted the data with bi-diffusion model, which indicates contribution of two species in the diffusion model. We got large diffusion time at these concentrations pointing out that the size (r_H) of the diffusing particle is large which may be due to the large aggregate formation of cytochrome c.[35] From 58% ethanol concentration, we got such large aggregates of cytochrome c. The aggregate formation may occur due to intensive hydrophobic interaction of ethanol with the protein.

3.3b *Fluorescence Correlation Spectroscopy (FCS)-Conformational Dynamics of AuNC-Cyt C*: Conformational dynamics was monitored using fluorescence correlation spectroscopy (FCS). For ethanol concentrations ranging from 0% (v/v) to 44.75% (v/v) there are two time scales of conformation dynamics as the FCS data was fitted to a model consisting of single component diffusion and two components of relaxation. Beyond these concentrations there is only one time scale of conformation dynamics as we have used equation (2) for fitting the data. Table 3 and Figure 6 summarize the τ_{R1} and τ_{R2} values for various concentrations of ethanol. It can be seen from Figures 6a and 6b that the values of τ_{R1} and τ_{R2} vary non-monotonically with increase in ethanol concentration (χ_{EtOH}, % v/v). They have an oscillatory dependence on the ethanol concentration, χ_{EtOH}.

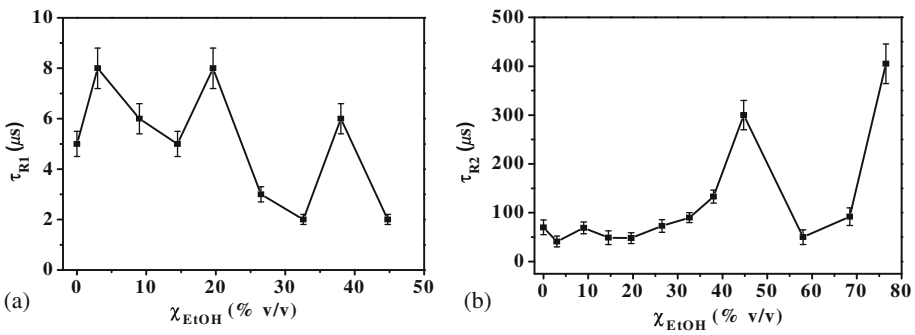

Figure 6. Variation of time scales of conformation dynamics (a) τ_{R1} and (b) τ_{R2} of Cyt C-AuNC in different concentrations of ethanol.

4. Conclusions

The most important finding of this work is the ethanol induced re-folding of Cyt C which is unfolded on binding to AuNC ($\chi_{EtOH} = 0\%$). The CD spectra reveal the refolding of protein on increase in the ethanol concentration. The refolding may occur due to two factors: (a) solvent environment change around the protein; and, (b) constraints arising due to the presence of gold nanoclusters inside the protein. MD simulation of systems containing AuNC is non-trivial. We will address this in our future work on Cyt C bound to AuNC.

Acknowledgments

Thanks are due to Department of Science and Technology, India (Centre for Ultrafast Spectroscopy and Microscopy Project and J C Bose Fellowship) and the Council of Scientific and Industrial Research (CSIR) for generous research support. C G and M A A thank CSIR for awarding fellowships.

References

1. Kwon K C, Ryu J H, Lee J H, Lee E J, Kwon I C, Kim K and Lee J 2014 Proteinticle/Gold Core/Shell Nanoparticles for Targeted Cancer Therapy without Nanotoxicity *Adv. Mater.* **26** 6436
2. Dreaden E C, Raji I O, Austin L A, Fathi S, Mwakwari S C, Humphries W H, Kang B, Oyelere A K and El-Sayed M A 2014 P-Glycoprotein-Dependent Trafficking of Nanoparticle-Drug Conjugates *Small* **10** 1719
3. Zheng C, Shao W, Paidi S K, Han B, Fu T, Wu D, Bi L, Xu W, Fan Z and Barman I 2015 Pursuing shell-isolated nanoparticle-enhanced Raman spectroscopy (SHINERS) for concomitant detection of breast lesions and microcalcifications *Nanoscale* **7** 16960
4. Li M, Kang J W, Dasari R R and Barman I 2014 Shedding Light on the Extinction-Enhancement Duality in Gold Nanostar-Enhanced Raman Spectroscopy *Angew. Chem. Int. Ed.* **53** 14115
5. Lee Y K, Kim S and Nam J M 2015 Dark-Field-Based Observation of Single-Nanoparticle Dynamics on a Supported Lipid Bilayer for In Situ Analysis of Interacting Molecules and Nanoparticles *ChemPhysChem* **16** 77
6. Sun T, Zhang Y S, Pang B, Hyun D C, Yang M and Xia Y 2014 Engineered nanoparticles for drug delivery in cancer therapy *Angew. Chem. Int. Ed.* **53** 12320
7. Ghosh S, Das N K, Anand U and Mukherjee S 2015 Photostable Copper Nanoclusters: Compatible Förster Resonance Energy-Transfer Assays and a Nanothermometer *J. Phys. Chem. Lett.* **6** 1293
8. Stamplecoskie K G and Kamat P V 2014 Size-Dependent Excited State Behavior of Glutathione-Capped Gold Clusters and their Light-Harvesting Capacity *J. Am. Chem. Soc.* **136** 11093
9. Khandelia R, Bhandari S, Pan U N, Ghosh S S and Chattopadhyay A 2015 Gold Nanocluster Embedded Albumin Nanoparticles for Two-Photon Imaging of Cancer Cells Accompanying Drug Delivery *Small* **11** 4075
10. Zhu J, Liao L, Bian X, Kong J, Yang P and Liu B 2012 pH-controlled delivery of doxorubicin to cancer cells, based on small mesoporous carbon nanospheres *Small* **8** 2715
11. Wang C G, Chen J J, Talavange T and Irudayaraj J 2009 Gold nanorod/Fe_3O_4 nanoparticle "nano-pearl-necklaces" for simultaneous targeting, dual-mode imaging, and photothermal ablation of cancer cells *Angew. Chem. Int. Ed.* **121** 2797
12. Chaudhari K, Xavier P L and Pradeep T 2011 Understanding the Evolution of Luminescent Gold Quantum Clusters in Protein Templates *ACS Nano* **5** 8816
13. Chattoraj S, Amin M A, Mohapatra S, Ghosh S and Bhattacharyya K 2016 Cancer Cell Imaging Using *In Situ* Generated Gold Nanoclusters *ChemPhysChem* **17** 61
14. Chattoraj S, Amin M A, Jana B, Mohapatra S, Ghosh S and Bhattacharyya K 2016 Selective Killing of Breast Cancer Cells by Doxorubicin-Loaded Fluorescent Gold Nanoclusters: Confocal Microscopy and FRET *ChemPhysChem* **17** 253
15. Wang Y, Chen J and Irudayaraj J 2011 Nuclear Targeting Dynamics of Gold Nanoclusters for Enhanced Therapy of $HER2^+$ Breast Cancer *ACS Nano* **5** 9718
16. Ding C and Tian Y 2015 Gold nanocluster-based fluorescence biosensor for targeted imaging in cancer cells and ratiometric determination of intracellular pH *Biosens. Bioelectron.* **65** 183
17. Gao S, Chen D, Li Q, Ye J, Jiang H, Amatore C and Wang X 2014 Near-infrared fluorescence imaging of cancer cells and tumors through specific biosynthesis of silver nanoclusters *Sci. Rep.* **4** 4384
18. Nguyen D H, Lee J S, Choi J H, Park K M, Lee Y and Park K D 2016 Hierarchical self-assembly of magnetic nanoclusters for theranostics: Tunable size, enhanced magnetic resonance imagability, and controlled and targeted drug delivery *Acta Biomater.* **35** 109
19. Chattoraj S, Amin M A and Bhattacharyya K 2016 Cytochrome c-Capped Fluorescent Gold Nanoclusters: Imaging of Live Cells and Delivery of Cytochrome c *ChemPhysChem* **17** 2088
20. Ghosh P, Yang X, Arvizo R, Zhu Z J, Agasti S S, Mo Z and Rotello V M 2010 Intracellular Delivery of a Membrane-Impermeable Enzyme in Active Form Using Functionalized Gold Nanoparticles *J. Am. Chem. Soc.* **132** 2642
21. Liu C L, Wu H T, Hsiao Y H, Lai C W, Shih C W, Peng Y K, Tang K C, Chang H W, Chien Y C, Hsiao J K, Cheng J T and Chou P T 2011 Insulin-directed synthesis of fluorescent gold nanoclusters: Preservation of insulin bioactivity and versatility in cell imaging *Angew. Chem. Int. Ed.* **50** 7056
22. Li K, Li Y, Shelton J M, Richardson J A, Spencer E, Chen Z J, Wang X and Williams R S 2000 Cytochrome c deficiency causes embryonic lethality and attenuates stress-induced apoptosis *Cell* **101** 389

23. Liu X, Kim C N, Yang J, Jemmerson R and Wang X 1996 Induction of apoptotic program in cell-free extracts: Requirement for dATP and cytochrome c *Cell* **86** 147
24. Ghosh R, Roy S and Bagchi B 2014 Multidimensional free energy surface of unfolding of HP-36: Microscopic origin of ruggedness *J. Chem. Phys.* **141** 135101
25. Roy S, Jana B and Bagchi B 2012 Dimethyl sulfoxide induced structural transformations and non-monotonic concentration dependence of conformational fluctuation around active site of lysozyme *J. Chem. Phys.* **136** 115103
26. Chattoraj S, Mandal A K and Bhattacharyya K 2014 Effect of ethanol-water mixture on the structure and dynamics of lysozyme: A fluorescence correlation spectroscopy study *J. Chem. Phys.* **140** 115105
27. Amin M A, Halder R, Ghosh C, Jana B and Bhattacharyya K 2016 Effect of alcohol on the structure of cytochrome C: FCS and molecular dynamics simulations *J. Chem. Phys.* **145** 235102
28. Mojumdar S S, Chowdhury R, Chattoraj S and Bhattacharyya K 2012 Role of Ionic Liquid on the Conformational Dynamics in the Native, Molten Globule, and Unfolded States of Cytochrome C: A Fluorescence Correlation Spectroscopy Study *J. Phys. Chem. B* **116** 12189
29. Haldar S, Mitra S and Chattopadhyay K 2010 Role of Protein Stabilizers on the Conformation of the Unfolded State of Cytochrome c and its Early Folding Kinetics Investigation at Single Molecular Resolution *J. Biol. Chem.* **285** 25314
30. Ghosh S, Mandal U, Adhikari A and Bhattacharyya K 2009 Study of Diffusion of Organic Dyes in a Triblock Copolymer Micelle and Gel by Fluorescence Correlation Spectroscopy *Chem. Asian J.* **4** 948
31. Enderlein J, Gregor I, Patra D, Dertinger T and U B Kaupp 2005 Performance of fluorescence correlation spectroscopy for measuring diffusion and concentrations *ChemPhysChem* **6** 2324
32. Sherman E, Itkin A, Kuttner Y Y, Rhoades E, Amir D, Haas E and Haran G 2008 Using Fluorescence Correlation Spectroscopy to Study Conformational Changes in Denatured Proteins *Biophys. J.* **94** 4819
33. Chattopadhyay K, Saffarian S, Elson E L and Frieden C 2005 Measuring Unfolding of Proteins in the Presence of Denaturant Using Fluorescence Correlation Spectroscopy *Biophys. J.* **88** 1413
34. Myer Y P 1968 Far Ultraviolet Circular Dichroism Spectra of Cytochrome C *Biochim. Biophys. Acta* **154** 84
35. Haldar S, Sil P, Thangamuniyandi M and Chattopadhyay K 2015 Conversion of Amyloid Fibrils of Cytochrome c to Mature Nanorods through a Honeycomb Morphology *Langmuir* **31** 4213
36. Balakrishnan G, Hu Y, Oyerinde O F, Su J, Groves J T and Spiro T G 2007 A Conformational Switch to β-Sheet Structure in Cytochrome c Leads to Heme Exposure. Implications for Cardiolipin Peroxidation and Apoptosis *J. Am. Chem. Soc.* **129** 504
37. Kubelca J, Hofrichter J and Eaton W A 2004 The protein folding 'speed limit' *Curr. Opin. Struct. Biol.* **14** 76
38. Choi J, Kim S, Tachikawa T, Fujitsuka M and Majima T 2011 pH-Induced Intramolecular Folding Dynamics of i-Motif DNA *J. Am. Chem. Soc.* **133** 16146
39. Pabbathi A, Ghosh S and Samanta A 2013 FCS study of the structural stability of lysozyme in the presence of morpholinium salts *J. Phys. Chem. B* **117** 16587
40. Han Y, He D S, Liu Y, Xie S, Tsukuda T and Li Z Y 2012 Size and Shape of Nanoclusters: Single-Shot Imaging Approach *Small* **8** 2361